

Cite this: *Chem. Sci.*, 2021, 12, 13909

All publication charges for this article have been paid for by the Royal Society of Chemistry

# Lipid-mimicking phosphorus-based glycosidase inactivators as pharmacological chaperones for the treatment of Gaucher's disease†

Manuel Scherer,<sup>‡a</sup> Andrés G. Santana,<sup>ID ‡a</sup> Kyle Robinson,<sup>a</sup> Steven Zhou,<sup>b</sup> Hermen S. Overkleeft,<sup>ID c</sup> Lorne Clarke<sup>b</sup> and Stephen G. Withers<sup>ID \*a</sup>

Gaucher's disease, the most prevalent lysosomal storage disorder, is caused by missense mutation of the GBA gene, ultimately resulting in deficient GCCase activity, hence the excessive build-up of cellular glucosylceramide. Among different therapeutic strategies, pharmacological chaperoning of mutant GCCase represents an attractive approach that relies on small organic molecules acting as protein stabilizers. Herein, we expand upon a new class of transient GCCase inactivators based on a reactive 2-deoxy-2-fluoro- $\beta$ -D-glucoside tethered to an array of lipid-mimicking phosphorus-based aglycones, which not only improve the selectivity and inactivation efficiency, but also the stability of these compounds in aqueous media. This hypothesis was further validated with kinetic and cellular studies confirming restoration of catalytic activity in Gaucher cells after treatment with these pharmacological chaperones.

Received 13th July 2021  
Accepted 17th September 2021

DOI: 10.1039/d1sc03831a

rsc.li/chemical-science

## Introduction

Gaucher's disease<sup>1</sup> is a genetic condition resulting from deficiency of the lysosomal enzyme  $\beta$ -glucocerebrosidase (GCCase EC: 4.2.1.25) with the concomitant accumulation of glucosylceramide. The deficiency of GCCase is a consequence of a large number of individual variants within the GBA gene and the resultant clinical features of Gaucher's disease are heterogeneous even when patients share the same pathogenic variant.<sup>2</sup> The recent population-based studies showing that GBA variants are over-represented in Parkinson disease patients has expanded the role and medical impact of GCCase deficiency.<sup>3</sup> A frequent mechanism underlying GCCase deficiency is protein misfolding resulting in intracellular instability and altered subcellular trafficking. This has been aptly demonstrated for the two common GBA missense variants N370S (p.N409S) and L444P (p.L483P).<sup>4</sup> Currently approved therapies for Gaucher's disease include enzyme replacement, effective only for the non-neuronal forms of the disease, as well as substrate-reduction therapy. Pharmacological chaperones (PCs) represent an additional potential therapeutic approach allowing the targeting of

both systemic and neurological symptoms. This form of treatment utilizes small molecules, most commonly GCCase competitive inhibitors, to promote and stabilize the folded conformation of mutant GCCase,<sup>5</sup> thereby assisting successful transit to the lysosome.<sup>6</sup> While a number of potential chaperones have been evaluated, none have yet received clinical approval for the treatment of Gaucher's disease. The vast majority of GCCase PCs developed to date have been reversible competitive inhibitors. *In vitro* studies have shown that these PCs increase the quantity of GCCase within cells but suffer from prolonged inhibition of the enzyme within the lysosome. This is further exacerbated by the basic, lysosomotropic properties of these compounds. Potential means to avert this issue include development of reversible, non-competitive GCCase ligands,<sup>7</sup> as well as ligands that can be actively cleaved by GCCase once it is correctly targeted to the lysosome. An alternative approach proposed by our group and others involves the generation of molecules that utilize the catalytic mechanism of GCCase to form a transient covalent intermediate with the enzyme and subsequently undergo cleavage within the lysosome to release the active enzyme.<sup>8</sup> To be successful as a therapeutic, the kinetics of this process require fine tuning. A major advantage of such an approach is that although the parent molecule is a potent GCCase inhibitor, the cleaved and released end product will have no significant affinity for the active site. 2-Fluoroglucosides (2FGlc) with activated leaving groups are excellent candidates since they form a long-lived, but catalytically competent glycosyl-enzyme intermediate with retaining  $\beta$ -glycosidases such as GCCase (Fig. 1).<sup>9</sup> Early studies utilizing purified GCCase showed that 2-deoxy-2-fluoro- $\beta$ -D-glucosyl fluoride (2FGLcF) forms a 2-

<sup>a</sup>Dept. of Chemistry, University of British Columbia, Vancouver, British Columbia, V6T 1Z1, Canada. E-mail: withers@chem.ubc.ca

<sup>b</sup>Dept. of Medical Genetics, University of British Columbia, Vancouver, British Columbia, V6H 3N1, Canada

<sup>c</sup>Institute of Chemistry, Leiden University, Leiden, Netherlands

† Electronic supplementary information (ESI) available: Synthetic methods, NMR characterization, GCCase inactivation kinetics. See DOI: 10.1039/d1sc03831a

‡ These authors contributed equally to this work.



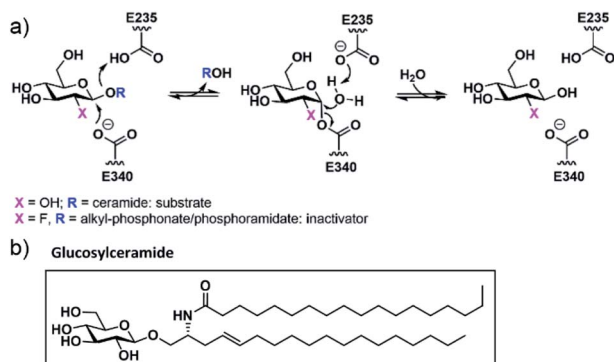


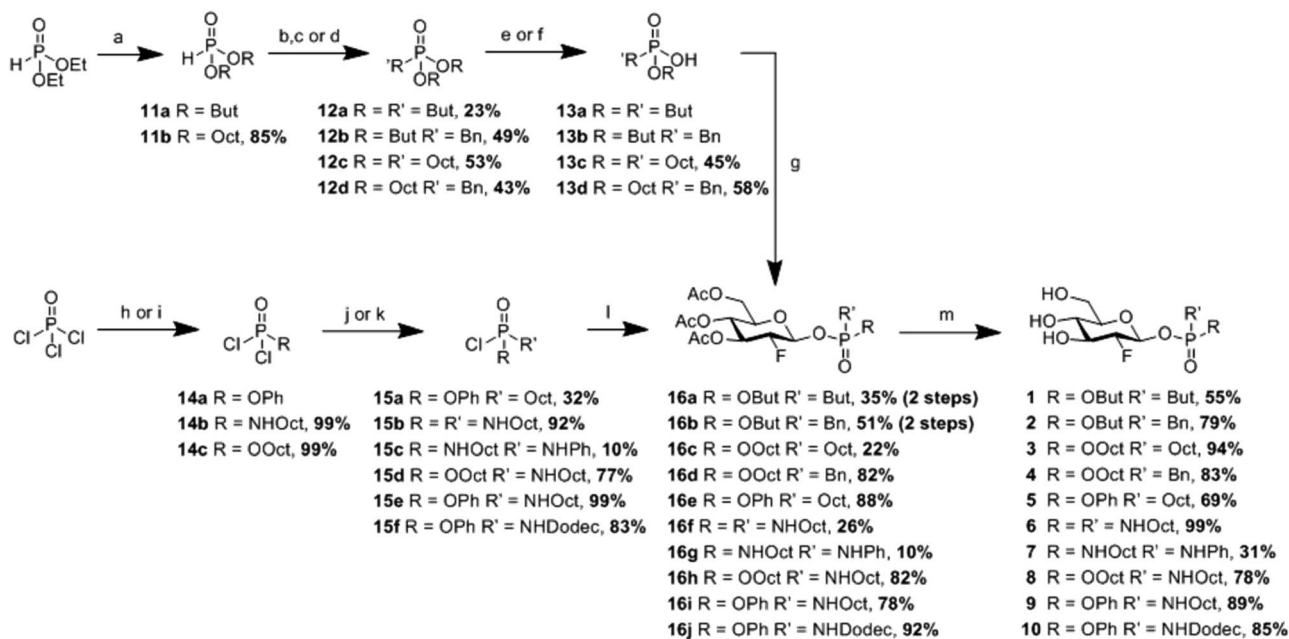
Fig. 1 (a) GCase double-displacement mechanism acting on its natural substrate or a 2FGlc-derived inactivator; (b) chemical structure of glucosylceramide, GCase natural substrate.

fluoroglucosyl-enzyme intermediate with a hydrolytic half-life of 1300 min and, when administered to rats, this molecule inactivates GCase in all organs, including the brain.<sup>10</sup> These bio-distribution and release kinetics are ideal, but the rate constant for GCase inactivation was found to be too low to be clinically useful. This has led to two separate approaches to potentially increase this rate constant. One involves replacement of the fluoride leaving group with an imidate that can be activated by protonation in the active site.<sup>11</sup> The other involves replacement with a dialkyl phosphate leaving group in which the

hydrophobic alkyl residues mimic the ceramide of the natural substrate glucosylceramide (Fig. 1), while the low  $pK_a$  of the aglycone ensures rapid inactivation. Indeed, inactivation rates were >4000-fold higher than those of 2FGlcF, and with much greater selectivity over other glycosidases. Unfortunately, the dialkyl phosphates were unstable, with a half-life of *ca.* 15 min under physiological conditions. In order to minimize instability, a single phosphonate analogue bearing *O*-benzyl and *C*-benzyl substituents was synthesized and shown to indeed be more stable ( $t_{1/2}$  = 630 min) but was a less efficient GCase inactivator.<sup>8b</sup> Based on these proof of principle observations, we set out to find more stable and more active chaperones by exploring other phosphonate substituents that better mimic the natural substrate, along with the use of phosphoramidates and phosphordiamidates as leaving groups that may recruit additional stabilizing interactions through their nitrogen atom.

## Results and discussion

Syntheses of the phosphorus-based aglycones and their 2FGlc-phosphonates, phosphordiamidates and phosphoramidates are shown in Scheme 1. 2FGlc phosphonates **1–4** were prepared *via* Koenigs-Knorr glycosylation of 3,4,6-tri-*O*-acetyl-2-deoxy-2-fluoro- $\alpha$ -D-glucopyranosyl bromide with the respective phosphonic acid mono esters **13a–13d**. The glycosylation products **16a–16d** were subsequently de-*O*-acetylated under methoxide-



Scheme 1 Synthesis of 2-fluoroglucosyl phosphorus-based aglycones: (a) **11b**: diethyl phosphite, *n*-octanol, NaH, 160 °C; (b) **11a**, NaH, THF, alkyl halide, **12a**: with *n*-butyl iodide, **12b**: with BnBr; (c) **12c**: **11b**, Na, toluene, 1-bromooctane, reflux; (d) **12d**: **11b**, Cs<sub>2</sub>CO<sub>3</sub>, DMF, BnBr, TBAl; (e) **13a**, **13b** and **13d**: TMSI, CH<sub>2</sub>Cl<sub>2</sub>; (f) **13c**: NaI, pyridine, reflux; (g) 3,4,6-tri-*O*-acetyl-2-deoxy-2-fluoro- $\alpha$ -D-glucopyranosyl bromide, THF/MeCN/CH<sub>2</sub>Cl<sub>2</sub> or MeCN, Ag<sub>2</sub>CO<sub>3</sub> **16a**: from **13a**, **16b**: from **13b**, **16c**: from **13c**, **16d**: from **13d**; (h) **14b**: *n*-octylamine, Et<sub>3</sub>N, toluene; (i) **14c**: *n*-octanol, quant.; (j) **15a**: from **14a** with *n*-octylmagnesium bromide, Et<sub>2</sub>O/toluene (4 : 1); (k) Et<sub>3</sub>N, toluene, corresponding amine **15b**: POCl<sub>3</sub>, *n*-octylamine, **15c**: from **14b** with aniline, **15d**: from **14c** with *n*-octylamine, **15e**: from **14a** with *n*-octylamine; **15f**: from **14a** with *n*-dodecylamine; (l) 3,4,6-tri-*O*-acetyl-2-deoxy-2-fluoro- $\alpha$ -D-glucopyranose, CH<sub>2</sub>Cl<sub>2</sub>, Et<sub>3</sub>N, 3 Å molecular sieves, **16e**: from **15a**, **16f**: from **15b**, **16g**: from **15c**, **16h**: from **15d**, **16i**: from **15e**, **16j**: from **15f**; (m) Na, MeOH, **1**: from **16a**, **2**: from **16b**, **3**: from **16c**, **4**: from **16d**, **5**: from **16e**, **6**: from **16f**, **7**: from **16g**, **8**: from **16h**, **9**: from **16i**, **10**: from **16j**; compounds **11a** and **14a** are commercially available.



catalyzed conditions to furnish the desired inactivators **1–4**. The acceptor phosphonic acid mono esters themselves (**13a–13d**) were readily synthesized from dialkyl phosphites **11a** and **11b** which, after alkylation, gave dialkyl alkylphosphonates **12a–12d**. Finally, the use of either TMSI or NaI allowed the transformation of dialkyl alkylphosphonates **12a–12d** into the corresponding phosphonic acid mono esters **13a–13d**. 2FGlc phosphonate **5** was prepared from commercially available POCl<sub>2</sub>Ph onto which an octyl residue had been attached using Grignard conditions to give octyl phenyl-phosphoryl chloride **15a**. Coupling of chloride **15a** with 3,4,6-tri-*O*-acetyl-2-fluoro-*D*-glucopyranose using Et<sub>3</sub>N provided per-*O*-acetylated glycosyl phosphonate **16e** from which compound **5** was readily obtained by deprotection. Compounds **1–5**, thus prepared, were evaluated as diastereomeric mixtures. Next, to check whether the phosphorus chirality in these diastereomeric compounds has any significant effect on the binding affinity towards the enzyme, a sample of **4** was subjected to stringent chromatography (see ESI†) yielding a 40 : 1 ratio of the two phosphorus diastereomers. With a *k*<sub>i</sub>/*K*<sub>i</sub> value of 40.9 min<sup>-1</sup> mM<sup>-1</sup>, the inactivation rate of this highly enriched fraction was only 1.1-fold greater than that of the 50 : 50 mixture of **4**, indicating that the two stereoisomers bind the enzyme active site with very similar affinities.

Evaluation of the 2FGlc phosphonates **1–5** (Fig. 2) as inactivators of GCCase revealed a trend wherein increasing the hydrophobicity of the aglycone resulted in faster inactivation of GCCase. This is presumably a consequence of the substrates becoming closer mimics of ceramide with its long hydrophobic chains (Fig. 1). Interestingly, and as seen previously, the presence of an aromatic residue is beneficial for the inactivation since octyl-benzyl derivative **4** was three times more active than the di-octyl analogue **3** (36.4 min<sup>-1</sup> mM<sup>-1</sup> for **4** vs. 10.9 min<sup>-1</sup> mM<sup>-1</sup> for **3**) (Table 1). As a consequence of this trend, there is

Table 1 Inactivation kinetics<sup>a</sup>

	<i>k</i> <sub>i</sub> [min <sup>-1</sup> ]	<i>K</i> <sub>i</sub> [μM]	<i>k</i> <sub>i</sub> / <i>K</i> <sub>i</sub> [min <sup>-1</sup> mM <sup>-1</sup> ]
<b>1</b> R = OBut R' = But	0.49	264	1.87
<b>2</b> R = OBut R' = Bn	5.44	742	7.34
<b>3</b> R = OOct R' = Oct	4.09	377	10.9
<b>4</b> R = OOct R' = Bn	3.67	101	36.4
<b>5</b> R = OPh R' = Oct	18.6	117	160
<b>6</b> R = R' = NHOct	0.13	8.2	16.1
<b>7</b> R = NHOct R' = NHPH	0.1	4.8	21.5
<b>8</b> R = OOct R' = NHOct	7.45	188	39.5
<b>9</b> R = OPh R' = NHOct	15	36.2	416
<b>10</b> R = OPh R' = NHDodec	4.22	22.2	190

<sup>a</sup> 37 °C, pH = 5.5 (for detailed procedure, see ESI).

an almost 20-fold increase of the second-order rate constant *k*<sub>i</sub>/*K*<sub>i</sub> in going from the di-butyl derivative **1** to the octyl-benzyl analogue **4**, even though their substituent inductive effects must be similar. Importantly, however, by altering the position of the oxygen atom (**4** to **5**), the rate constant *k*<sub>i</sub> can be further increased 5-fold (3.67 min<sup>-1</sup> for **4** vs. 18.6 min<sup>-1</sup> for **5**) while the *K*<sub>i</sub> stays largely unaffected (101 μM for **4** vs. 117 μM for **5**), pushing the *k*<sub>i</sub>/*K*<sub>i</sub> value up to 160 min<sup>-1</sup> mM<sup>-1</sup> (Table 1). The rise in this case is presumably a consequence of the greater electronegativity of the phenol (*pK*<sub>a</sub> ~ 10) than the alkyl alcohol it replaced (*pK*<sub>a</sub> ~ 15).

While the improvements achieved here were useful and in the right direction, we were intrigued by the possibilities of incorporating nitrogen atoms into the anomeric leaving group, not only because it would render closer mimics of the natural aglycone, glucosylceramide (Fig. 1), but also because of the potential of harnessing strong hydrogen bonding interactions with active site carboxylic acids, a strategy behind the impressive history of azasugar inhibitors of glycosidases. An added bonus is the built-in acid lability of phosphoramidates, minimising persistence in the lysosome through enhanced spontaneous hydrolysis.<sup>12</sup> Fittingly, 2FGlc phosphordiamidates **6–7** were synthesized by a similar approach to that used for the phosphonates (Scheme 1). Coupling of the fluorinated glycone and aglycone moieties was achieved by reaction of phosphordiamidochloridates **15b** and **15c** with the anomeric hemiacetal of the otherwise protected 2FGlc to give intermediates **16f** and **16g**. The excellent β-selectivity observed presumably arose from the greater reactivity of the less sterically hindered beta anomer, followed by rapid interconversion of the alpha and beta anomers under the employed reaction conditions. These intermediates were subsequently deacetylated to provide 2FGlc phosphordiamidates **6–7** (Fig. 2). In parallel, 2FGlc phosphoramidates **8–10** were obtained in excellent overall yields of 49% up to 76% from commercially available POCl<sub>3</sub> and POCl<sub>2</sub>OPh in three and four synthetic steps, respectively (Scheme 1). The approach involved the preparation of phosphoryldichlorides **14a–14c** which were transformed into

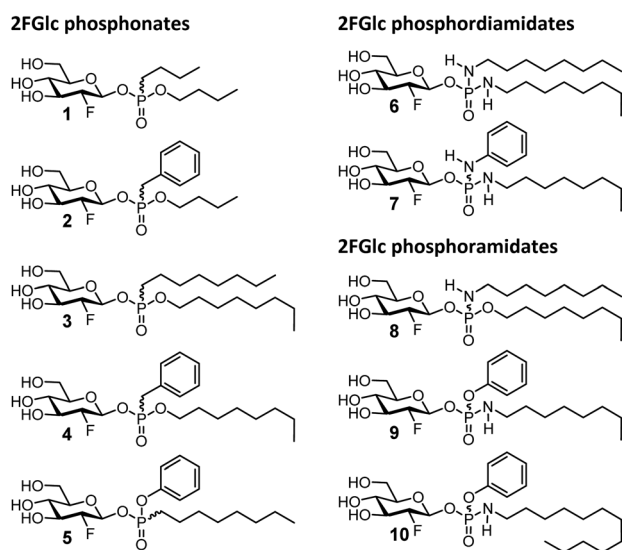


Fig. 2 Glucosylceramide-mimicking 2-deoxy-2-fluoroglucopyranosyl phosphonates, phosphoramidates and phosphordiamidates **1–10** prepared in this study.



phosphoramidochloridates **15d–15f**. Subsequent highly  $\beta$ -selective and high yielding anomeric phosphorylations provided compounds **16h–16j**. These afforded 2FGlc phosphoramidates **8–10** after Zemplén deprotection (Fig. 2). Except for compounds **4** and **6**, all final compounds were obtained as a 1 : 1 mixture of diastereomers at the phosphorus stereocenter and were enzymatically evaluated as such.

Consistent with expectations about improved binding, the 2FGlc phosphordiamidates **6** and **7** both proved to bind with high affinity, exhibiting  $K_i$  values of 8.2  $\mu\text{M}$  and 4.8  $\mu\text{M}$ , respectively. However, it appears that this high affinity derives from ground state binding since inactivation rates were also low, as reflected in the  $k_i$  values of 0.13  $\text{min}^{-1}$  and 0.10  $\text{min}^{-1}$  and modest second-order rate constants of  $k_i/K_i = 16.1 \text{ min}^{-1} \text{ mM}^{-1}$  for **6** and 21.5  $\text{min}^{-1} \text{ mM}^{-1}$  for **7** (Table 1). In order to speed up the inactivation step, we elected to replace one of the amines on the phosphorus atom with a more electron-withdrawing *O*-alkyl or *O*-phenyl substituent in the form of the 2FGlc phosphoramidates **8–10**. The *N*-octyl-*O*-octyl reagent **8** did indeed bind better and react faster than the di-*O*-octyl derivative **3**, even though the effect was a modest 4-fold increase in  $k_i/K_i$ . However, by replacing the *O*-octyl with an *O*-Ph residue (compound **9**), the  $k_i$  value was increased and the  $K_i$  decreased resulting in a substantially higher second-order rate constant  $k_i/K_i$  of 416  $\text{min}^{-1} \text{ mM}^{-1}$ . Compound **9** combines the positive effects of the enhanced binding by the N-H (lowering the  $K_i$ ), the interaction of the aromatic residue and the electron-withdrawing nature of the OPh (enhancing  $k_i$ ). In an attempt to further increase the  $k_i/K_i$  value, the alkyl chain length of **9** was elongated from an *n*-octyl to an *n*-dodecyl residue (compound **10**), but surprisingly, this actually decreased the second-order rate constant two-fold (Table 1). Quite possibly the longer alkyl chains promote the formation of aggregates making compound **10** less accessible to the enzyme. Unsurprisingly, the isomer of compound **8** in which the nitrogen atom replaces the glycosidic oxygen (octyl 2FGlc-phosphoramidate) exhibited a very low affinity for the enzyme and behaved as a poor competitive inhibitor, rather than as an inactivator (synthesis in ESI†).

In order to test stability under physiological conditions, 2FGlc phosphoramidate **9** was incubated at 37 °C in a phosphate buffer at pH 6.8 and the decrease of the rate constant of inactivation due to degradation of the inactivator was followed over time and used as an indirect measure of the remaining inactivator concentration. Under these conditions, 2FGlc phosphoramidate **9** showed a similar rate of hydrolysis and half-life as the previously synthesized 2FGlc phosphonate (0.0014  $\text{min}^{-1}$  vs. 0.0011  $\text{min}^{-1}$  and  $t_{1/2}$  of 510 min vs. 630 min, respectively) and around 40 times enhanced stability compared to the original 2FGlc phosphates ( $t_{1/2}$  510 min vs. 15 min) (see ESI, Fig. S3†).<sup>8b</sup>

The pharmacological chaperone potential of this class of compounds was tested with phosphonate **4** as a representative molecule, since we know that phosphorus chirality is not a significant factor in determining affinity in this case. Mouse embryonic fibroblast (MEF) cells from transgenic mice expressing solely human L444P-containing GCCase (a common

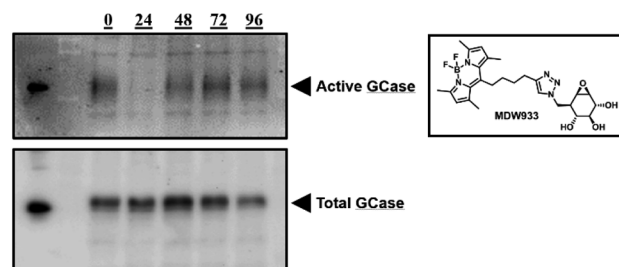


Fig. 3 PAGE gels imaged with the fluorescent activity-based probe MDW933 (top) and Western blot (bottom), showing changes in active and total [GCCase] over time (h) after treatment with phosphonate **4**, respectively. Lane 0 represents untreated cells.

variant underlying neuropathic Gaucher's disease) on a murine GCCase knockout background<sup>13</sup> were continuously treated for three days with daily media changes containing 100  $\mu\text{M}$  2FGlc phosphonate **4**. After the three days, cells were washed, fresh media without inactivator was added and cells subsequently harvested at various time intervals. To assess the amounts of rescued active enzyme present, we used the fluorescent mechanism-based inactivator MDW933 that reacts only with active enzyme (Fig. 3).<sup>14</sup> By running PAGE gels we can assess the amount of reactivated enzyme present from the intensity of the fluorescence, while subsequent Western blots of the same gel give insights into total mass of enzyme present. Total enzyme gradually increased to a maximum at 48 hours (Fig. 3, bottom), then appears to decrease. By contrast, relatively little active GCCase is seen after 24 hours due to inactivation by the chaperone, but then it gradually increases to an apparent maximum at 48–72 hours due to steady reactivation through turnover of the 2-fluoroglucosyl enzyme (Fig. 3, top). In parallel both the GCCase and hexosaminidase activities of the cells were measured during the four days after completion of treatment. Consistent with the pattern seen in the gels, activity increased over time, reaching 1.31 times the initial activity after 96 hours (see ESI, Table S1†). To account for variations in cell sampling all values were normalized relative to the hexosaminidase activity measured.<sup>7</sup>

Similar results were obtained on the same system with a dosing regimen involving treatment for 7 days, then monitoring for activity and protein concentration *via* MDW933 labelling and Western blots of PAGE gels, respectively (see ESI, Fig. S4†). This chaperone is also seen in patient fibroblast cells expressing the L444P mutation, as seen in Table S2.† Essentially equivalent levels of chaperoning are seen as with in MEF cells. Finally, this behaviour is not restricted to the L444P mutation since studies of the N370S mutant in both MEF cells and in human fibroblasts revealed similar profiles of activity gain as seen in the MDW933 stained gels of Fig. S5.†

These results therefore confirm that the 2FGlc phosphonate **4** is indeed able to: (1) penetrate the fibroblast cells, and (2) inactivate GCCase effectively. Fittingly, the recovery of the enzymatic activity seen over the course of seven days, due to gradual turnover of the covalently bound 2FGlc, is compatible with clinical practice.



## Conclusions

In conclusion, ten novel 2FGlc glycosides with different phosphorus-based aglycones were prepared and their inactivation potential towards GCCase analyzed. The 2FGlc phosphoramidate **9** proved to be a potent inactivator with a  $k_i/K_i$  value of  $416 \text{ min}^{-1} \text{ mM}^{-1}$  and was much more stable than the 2FGlc phosphates under physiological conditions. Cell assays confirmed that 2FGlc glycosides such as **4** are able to inactivate GCCase in fibroblast cells and that the inactivated enzyme slowly recovers activity on a timescale compatible with treatment, making them promising candidates as pharmacological chaperones.

## Data availability

All data are included.

## Author contributions

Manuel Scherer and Andrés G. Santana performed all the synthesis and most of the kinetic analyses. Kyle Robinson performed some of the enzyme kinetic studies. Steven Zhou performed cell-based analyses, supervised by Lorne Clarke. Hermen Overkleeft generated the fluorescent activity based probe. Funding was acquired by Lorne Clarke and Stephen G. Withers. Manuscript writing was performed primarily by MS, AGS and SGW with input from LC.

## Conflicts of interest

There are no conflicts to declare.

## Acknowledgements

We acknowledge financial support from the Canadian Institutes for Health Research (CIHR) and the Canadian Glycoscience Network GlycoNet. AGS would like to thank EMBO for a long-term postdoctoral fellowship (ALTF 1029-2013). MS thanks the Swiss National Science Foundation (SNSF) for a postdoctoral fellowship.

## Notes and references

- 1 A. H. Futerman and G. van Meer, *Nat. Rev. Mol. Cell Biol.*, 2004, **5**, 554.
- 2 P. K. Mistry, G. López, R. Schiffmann, N. W. Barton, N. J. Weinreb and E. Sidransky, *Mol. Genet. Metab.*, 2017, **120**, 8.
- 3 (a) F. Atashrazm, D. Hammond, G. Perera, C. Dobson-Stone, N. Mueller, R. Pickford, W. Scott Kim, J. B. Kwok, S. J. G. Lewis, G. M. Halliday and N. Dzamko, *Sci. Rep.*, 2018, **8**, 15446; (b) M. Horowitz, D. Elstein, A. Zimran and O. Goker-Alpan, *Hum. Mutat.*, 2016, **37**, 1121.
- 4 G. A. Grabowski, *Lancet*, 2008, **372**, 1263.
- 5 (a) R. Thomas and A. R. Kermode, *Mol. Genet. Metab.*, 2019, **126**, 83; (b) J. M. Benito, J. M. García Fernández and C. O. Mellet, *Expert Opin. Ther. Pat.*, 2011, **21**, 885.
- 6 D. Reczek, M. Schwake, J. Schroder, H. Hughes, J. Blanz, X. Y. Jin, W. Brondyk, S. Van Patten, T. Edmunds and P. Saftig, *Cell*, 2007, **131**, 770.
- 7 (a) E. D. Goddard-Borger, M. B. Tropak, S. Yonekawa, C. Tysoe, D. J. Mahuran and S. G. Withers, *J. Med. Chem.*, 2012, **55**, 2737; (b) M. Aguilar-Moncayo, M. I. García-Moreno, A. Trapero, M. Egido-Gabas, A. Llebaria, J. M. García Fernández and C. Ortiz Mellet, *Org. Biomol. Chem.*, 2011, **9**, 3698; (c) T. S. Rasmussen, S. Allman, G. Twigg, T. D. Butters and H. H. Jensen, *Bioorg. Med. Chem. Lett.*, 2011, **21**, 1519.
- 8 (a) C.-L. Kuo, W. W. Kallemeijn, L. T. Lelieveld, M. Mirzaian, I. Zoutendijk, A. Vardi, A. H. Futerman, A. H. Meijer, H. P. Spaink, H. S. Overkleeft, J. M. F. G. Aerts and M. Artola, *FEBS J.*, 2019, **286**, 584; (b) B. P. Rempel, M. P. Tropak, D. J. Mahuran and S. G. Withers, *Angew. Chem., Int. Ed.*, 2011, **50**, 10381.
- 9 S. C. Miao, J. D. McCarter, M. E. Grace, G. A. Grabowski, R. Aebersold and S. G. Withers, *J. Biol. Chem.*, 1994, **269**, 10975.
- 10 (a) J. D. McCarter, M. J. Adam, N. G. Hartman and S. G. Withers, *Biochem. J.*, 1994, **301**, 343; (b) C. P. Phenix, B. P. Rempel, K. Colobong, D. J. Doudet, M. J. Adam, L. A. Clarke and S. G. Withers, *Proc. Natl. Acad. Sci. U. S. A.*, 2010, **107**, 10842.
- 11 M. T. C. Walvoort, W. W. Kallemeijn, L. I. Willems, M. D. Witte, J. M. F. G. Aerts, G. A. van der Marel, J. D. C. Codée and H. S. Overkleeft, *Chem. Commun.*, 2012, **48**, 10386.
- 12 (a) I. Oney and M. Caplow, *J. Am. Chem. Soc.*, 1967, **89**, 6972; (b) T. Mena-Barragán, A. Narita, D. Matias, G. Tiscornia, E. Nanba, K. Ohno, Y. Suzuki, K. Higaki, J. M. García Fernández and C. Ortiz Mellet, *Angew. Chem., Int. Ed.*, 2015, **54**, 11696.
- 13 A. Sanders, H. Hemmelgarn, H. L. Melrose, L. Hein, M. Fuller and L. A. Clarke, *Blood Cells, Mol., Dis.*, 2013, **51**, 109.
- 14 M. D. Witte, W. W. Kallemeijn, J. Aten, K.-Y. Li, A. Strijland, W. E. Donker-Koopman, A. M. C. H. van den Nieuwendijk, B. Bleijlevens, G. Kramer, B. I. Florea, B. Hooibrink, C. E. M. Hollak, R. Ottenhoff, R. G. Boot, G. A. van der Marel, H. S. Overkleeft and J. M. F. G. Aerts, *Nat. Chem. Biol.*, 2010, **6**, 907.

